

Influence of P_2O_5 and SiO_2 addition on the phase, microstructure, and electrical properties of $KNbO_3$

S. Ullah^{1,2,*} · I. Ullah¹ · Y. Iqbal¹ · A. Manan^{1,3} · S. Ali¹ · A. Khan⁴

Received: July, 2018 / Accepted: —, 2018

Abstract In this contribution, the effect of P_2O_5 and SiO_2 addition on the phase, microstructure, and electrical properties of $KNbO_3$ was studied. Sample powders with the general formula $(1-x)KNbO_3 \cdot xP_2O_5$ ($x = 0.03, 0.05$) and $(1-x)KNbO_3 \cdot xSiO_2$ ($x = 0.1$) were prepared via mixed-oxide route. The thermal behavior of the mixed-milled powder was investigated by TG/DTA which revealed an overall weight loss of 33.4 wt % in the temperature range of $30 \leq T \leq 1200$ °C and crystallization exotherm occurring at about 795 °C. The present results indicated that P_2O_5 acted as a sintering aid and lowered the sintering temperature by about 30 °C and promoted densification of $KNbO_3$. Sample compositions at various stages of processing were characterized using X-ray diffraction. Samples sintered at $T \leq 1020$ °C revealed mainly $KNbO_3$ together with a couple of low-intensity K_3NbO_4 peaks as a secondary phase. The SEM images of $(1-x)KNbO_3 \cdot xSiO_2$ ($x = 0.1$) samples showed a slight increase in the average grain size from 3.76 μm to 3.86 μm with an increase in sintering temperature from 1000 °C to 1020 °C. Strong variations in dielectric constant and loss

tangent were observed due to P_2O_5 and SiO_2 addition as well as frequency of the applied AC signals.

Keywords Phase · Microstructure · Sintering · TG/DTA · Weight loss · Potassium niobate.

1 Introduction

To meet the massive demands of the evolving society advanced technological developments are required[1]. Therefore, it is highly desirable to use new and advanced materials with improved properties[2,3]. Currently, the lead-based piezoelectric materials, such as $Pb(Zr,Ti)O_3$ (PZT) and $Pb(Mg_{0.33}Nb_{0.67})O_3$ - $PbTiO_3$ (PMN-PT), dominate the commercial piezoelectric applications. While such materials, due their superior properties, have been widely used in microelectronics and electronic devices as dielectric capacitors, ultrasonic or medical transducers, ultrasonic motors, and sensors[4,5]. However, one of the major drawbacks of these materials is the environmental and health-related issues. These materials contain about 70 wt% of poisonous lead-oxide which is an ecological hazard[6]. Material scientists are looking forward to orient the current research towards environmentally friendly materials of comparable properties[7,8]. Recently, a number of materials such as barium titanate, bismuth-alkaline metal titanates, and alkaline-niobates are revisited as potential alternatives to lead-based piezoceramics[9].

Among those alternatives, potassium niobate [$KNbO_3$] (KN) based materials are the front-running candidates due to their large non linear optical[10] and electro-optic coefficient[11], moderate dielectric constant, and excellent photorefractive and electrical properties[12,13,14,15,16]. Additionally, such materials also offer possibilities for applications, for example, in the production of surface acoustic wave (SAW) devices and wide-band SAW filters[17,18]. However, the den-

Correspondence author: Dr. Saeed Ullah
E-mail: saeedullah.phy@gmail.com
Tel.: +92-342-9070068

1 Materials Research Laboratory, Department of Physics, University of Peshawar, 25120, Pakistan

2 Department of Physics, Gomal University, Dera Ismail Khan 29220, KP, Pakistan

3 Department of Physics, University of Science and Technology, Bannu Khyber Pakhtunkhwa, Pakistan

4 Center of Excellence in Solid State Physics, University of the Punjab, Lahore-54590, Pakistan

sification of these materials is problematic due to several reasons. One of the main reason is the phase stability of KNbO_3 which is limited to 1040°C which further restrains the high-temperature sintering[19]. Additionally, potassium oxide is volatile and evaporates easily with rising temperature during the sintering process and hence leads to the formation of some unstable secondary phases in the final product. Furthermore, slight changes in the stoichiometry can also result in the formation of unwanted phases.

Various techniques have been developed for the improvement of densification of niobate-based ceramics, for example, hot pressing and spark plasma sintering (SPS). However, these techniques are not suitable to enhance the sintering in various commercial applications[20,21]. Based on previous efforts, it has been concluded that the modification of stoichiometry[15] or addition of sintering agents such as CuO , CeO_2 , MnO_2 , TiO_2 and other oxides, have a significant impact on the improvement of sinterability[22,23,24,25,26,27,28,29]. These oxides form a liquid phase and promote densification[25,26,28].

The objective of the present work was to investigate the effect of P_2O_5 and SiO_2 addition on the phase, microstructure and electrical properties of KN. A number of experimental groups have reported the addition of various oxides into KN-based materials. However, to our knowledge, no report regarding the use of P_2O_5 and SiO_2 addition has, to date been appeared in the literature.

2 Materials and Experiment

The $(1-x)\text{KNbO}_3 \cdot x\text{P}_2\text{O}_5$ ($x = 0.03, 0.05$) and $(1-x)\text{KNbO}_3 \cdot x\text{SiO}_2$ ($x = 0.1$) samples were prepared via a conventional mixed-oxide route using K_2CO_3 and Nb_2O_5 as starting materials. The amount of oxides, to produce the stoichiometric KN, were calculated on the basis of their molecular weights. The weighed amounts were wet ball milled for 24 h in disposable polyethylene mill jars using Y-toughened ZrO_2 balls as grinding media and iso-propanol as a lubricant to make the slurry. The slurry was then dried overnight in an oven at 95°C . To determine the phase transformation temperatures, thermal gravimetry and differential thermal analysis (TG/DTA) was carried out in the temperature range of $30\text{-}1200^\circ\text{C}$ with a heating/cooling rate of $5^\circ\text{C}/\text{min}$ using a Perkin Elmer TG/DTA unit. The mix-milled powder was then calcined at 850°C for 2 h at the same heating/cooling rate. To lower the sintering temperature, the as-calcined powder were then mixed with 0.03 and 0.05 wt% P_2O_5 and 0.1 wt% SiO_2 and re-milled for 24 h.

The powders were then pressed into pellets of 10 mm diameters at ~ 100 MPa using a manual pellet press, followed by sintering at various temperatures. The apparent densities of the specimens were measured employing Archimedes

method, however, due to its hygroscopic nature, the P_2O_5 -added samples dissolved in water[30]. Densities were then calculated from the mass and dimensions of the pellets and converted to the relative densities using theoretical density (TD) of KNbO_3 ($4.167\text{ g}/\text{cm}^3$)[26].

The crystalline phases of compositions, at different stages of processing, were assessed by a JEOL X-ray diffractometer (model JDX-3532) in the 2θ range of $10\text{-}70^\circ$ with $\text{Cu } K\alpha$ radiations operating at 40 kV and 30 mA with a step size of 0.02° . The sintered samples were cut with a diamond fine cutting saw, smoothed using a polishing wheel with sandpaper and then polished using a polishing wheel with a nylon cloth and diamond paste. After polishing, the samples were thermally etched at a temperature 10% less than the corresponding sintering temperatures. Polished samples were then gold-coated to avoid charging in the scanning electron microscope (SEM). Microstructural characterization was performed using SEM (JEOL JSM 5910). The grain size measurements were performed using mean intercept length method at different areas of the sample. The dielectric constant (ϵ_r) and loss tangent ($\tan\delta$) were measured in a frequency range of 1 MHz to 1 GHz employing a 4287A LCR meter. All the experiments were carried out using the equipment installed at the Materials Research Laboratory (MRL) and Centralized Resource Laboratory (CRL), University of Peshawar.

3 Results and Discussions

3.1 TG/DTA Analysis

Fig. 1 depicts the TG/DTA curve of the stoichiometric precursor of KNbO_3 showing three major and two minor downward slopes in the employed temperature range i.e. from room temperature to 1200°C . Consistent with the TG slopes, four endotherms were observed on the DTA curve at temperatures $52\text{-}153^\circ\text{C}$, 464°C , 792°C and 1126°C respectively. The wt% losses determined at $50\text{-}171^\circ\text{C}$, $430\text{-}475^\circ\text{C}$ and $475\text{-}900^\circ\text{C}$ were 13.23 wt%, 4.28 wt%, and 11.11 wt% respectively. Furthermore, relatively minor wt% losses (i.e., 3.75 wt% and 1.052 wt%) were observed at $171\text{-}430^\circ\text{C}$ and $900\text{-}1200^\circ\text{C}$. The observed weight losses at different temperatures are listed in Table 1. The overall wt% loss was 33.4 wt%. The wt% loss at $50\text{-}171^\circ\text{C}$ may be due to the dehydration of the sample, i.e., the removal of surficial water present in the raw materials[31].

The weight loss observed in the temperature range $430\text{-}475^\circ\text{C}$ and the observed DTA endotherm at 464°C may be associated with the glass transition of some of the glass formers (i.e., P_2O_5 and SiO_2) present in the batch. In the temperature range of $475\text{-}900^\circ\text{C}$, the observed weight loss is attributed to the decomposition of K_2CO_3 , releasing CO_2

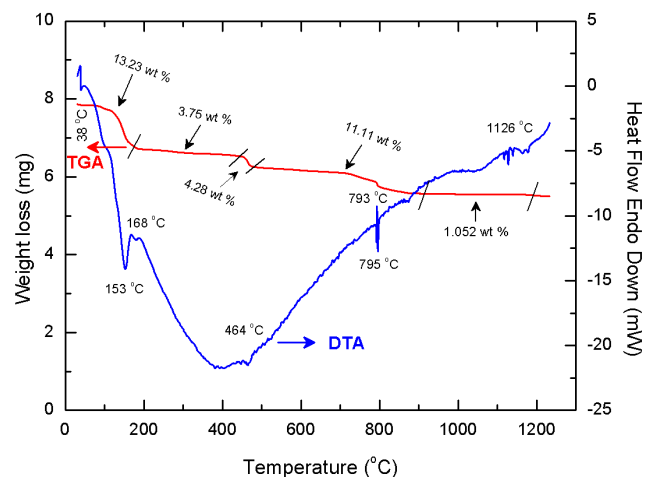
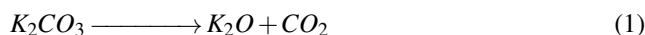


Fig. 1 TG/DTA curves of as-mixed-milled material, showing major weight losses in the temperature ranges of 50-171 °C, 430-475 °C and 475-900 °C with the corresponding endotherms at 153 °C, 464 °C and 792 °C. Note the corresponding endo-or exo-therms on the DTA curve.

by combustion reaction (See Eq. 1).



A corresponding endotherm was observed on the DTA curve at 792 °C. In the temperature range 900-1200 °C, the relatively small wt% loss is related to the removal of entrapped gases upon partial melting of the sample releasing CO₂ and other gases[32]. In the temperature range 900-1200 °C, the DTA curve showed a corresponding endotherm at 1126 °C consistent with the TG results. The exotherm observed on the DTA curve at 795 °C is associated with the crystallization of potassium niobate[33] as confirmed by phase analysis (See Fig. 2). Based on the TG/DTA analysis, temperatures in the range from 800 to 1030 °C were selected for calcinations. The mixed-milled sample was calcined in air at 850 °C for 2 h with a heating/cooling rate 5 °C/min.

Table 1 Weight loss of KNbO₃ at various temperatures.

S. No	Temperature range	Weight loss (mg)	Weight loss (%)
1	50 - 171 °C	1.04	13.23
2	171 - 430 °C	0.255	3.75
3	430 - 475 °C	0.280	4.28
4	475 - 900 °C	0.696	11.11
5	900 - 1200 °C	0.059	1.05

3.2 Phase Analysis

Fig. 2 shows the X-ray diffraction patterns of the as-mix-milled, calcined and sintered samples recorded at room temperature in the 2θ range of 10-70°. The d-spacings and relative intensities corresponding to the XRD peaks from the

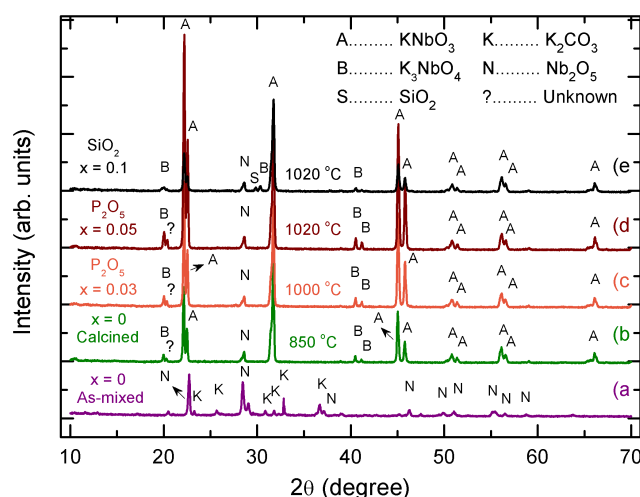


Fig. 2 X-ray diffraction patterns recorded from a) as-mix-milled batch b) (1-x)KNbO₃.xP₂O₅ (x = 0) calcined at 850 °C c) the (1-x)KNbO₃.xP₂O₅ (x = 0.03) sintered at 1000 °C d) the (1-x)KNbO₃.xP₂O₅ (x = 0.05) sintered at 1020 °C and e) the (1-x)KNbO₃.xSiO₂ (x = 0.1) sintered at 1020 °C.

as-mix-milled sample matched PDF # 70-292 for K₂CO₃ and PDF # 27-1312 for Nb₂O₅ labeled as "K" and "N" respectively which confirmed the presence of initial ingredients used in the present study. The XRD pattern of the (1-x)KNbO₃.xP₂O₅ (x = 0) sample, calcined at 850 °C for 2 h, is shown in Fig. 2(b). The d-spacings and relative intensities corresponding to major XRD peaks matched PDF # 32-0822 for KNbO₃ labeled as "A" which revealed the formation of KNbO₃ as a major phase; however, a couple of low-intensity peaks labeled as "K" and "N" matched PDF # 70-292 for K₂CO₃ and PDF # 27-1312 for Nb₂O₅ indicating incomplete reaction.

Fig. 2(c) and (d) show XRD patterns recorded from the (1-x)KNbO₃.xP₂O₅ (x = 0.03, x = 0.05) samples sintered at 1000 °C and 1020 °C respectively. The d-spacings and relative intensities corresponding to the major XRD peaks from (1-x)KNbO₃.xP₂O₅ (x = 0.03) compositions sintered at 1000 °C and (1-x)KNbO₃.xP₂O₅ (x = 0.05) sintered at 1020 °C matched the PDF # 32-0822 for KNbO₃ labeled as "A" which confirmed the occurrence of chemical reaction and hence the formation of KNbO₃ phase. A number of low-intensity peaks marked as "?" were also observed which could not be identified[26, 27, 28, 29].

Fig. 2(e) shows the XRD pattern recorded from the (1-x)KNbO₃.xSiO₂ (x = 0.1) sample sintered at 1020 °C. The corresponding d-spacings and relative intensities of XRD peaks matched the PDF # 32-0822 for KNbO₃ which confirmed the presence of KNbO₃ phase. For this composition, the unknown peak disappeared, however, an additional low-intensity peak marked as "S" appeared at 2θ = 29° which matched the PDF # 50-1431 for SiO₂. Additionally, the thermal treatment processes (such as calcination and sintering)

caused the emergence of secondary phases labeled as "B" (See Fig. 2(b-e)). The appearance of these peaks can be assigned to K_3NbO_4 (PDF # 52-1894) originating from the slight changes in the stoichiometry due to volatile alkaline oxides during the sintering process.

3.3 Density measurement

In the present work, the density of 3.07 g/cm^3 was measured for the as-mixed-milled sample, which is 73.6 % of the theoretical density of $KNbO_3$ [26]. The addition of 0.03 and 0.05 wt% P_2O_5 resulted in the densification of the material and hence enhanced the density by about 11.35 and 14.55 % of that of the mixed-milled sample. In addition, to increasing x value, the observed increase in density was caused by the rise of sintering temperature from 1000 to 1020 °C. Furthermore, the addition of 0.1 wt% SiO_2 lowered the density to 2.8 g/cm^3 (66.04 % of TD) which is reflected from the increase in grain size (See Sec. 3.4).

3.4 Microstructural Analysis

Fig. 3 depicts the secondary electron SEM images (SEIs) recorded from the thermally etched, gold-coated surfaces of $(1-x)KNbO_3 \cdot xSiO_2$ ($x = 0.1$). The microstructure comprised cubic and cuboidal grains with an average grain size of $3.76 \mu\text{m}$ and $3.86 \mu\text{m}$ along with agglomerates of fine grains in samples sintered at 1000 °C and 1020 °C for 2 h, respectively. Zhou et al.[34] reported that pure $KNbO_3$ has an average grain size of $2.5 \mu\text{m}$. Thus, the addition of SiO_2 caused an increase in the grain size of $KNbO_3$ ceramics which is evidenced by the reduction of the apparent density of the sample as commented above.

The composition analysis was carried out using energy dispersive X-ray spectroscopy (EDS). EDS detected the presence of K and Nb only in cubic and cuboidal grains with no Si. The agglomerates of fine grains contained K, Nb, and a small amount of Si. The EDS analysis (see table 2) detected 29.47 wt% K and 70.53 wt% Nb in the cubic grain labeled as "A", and 29.29 K wt% and 71.71 wt% Nb in cuboidal grains labeled as "C" (see Fig. 3(a,b)). Additionally, the agglomerates of fine grains marked as "B" revealed 29.29 wt%

Table 2 EDS-detected compositions of various grains.

Grains	Potassium (K %)	Niobium (Nb %)	Silicon (Si %)
A	29.47	70.53	-
B	29.29	69.09	1.62
C	29.29	71.71	-
D	29.33	70.67	-
E	28.62	65.28	6.10
F	29.87	71.13	-

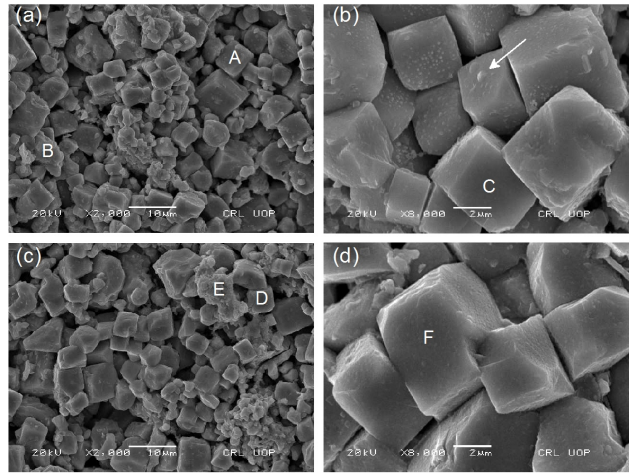


Fig. 3 Scanning electron micrographs of thermally etched gold-coated surface of $(1-x)KNbO_3 \cdot xSiO_2$ ($x = 0.1$) (a,b) sintered at 1000°C, showing the general microstructure grains of cubic and cuboidal morphology with an average grain size of $3.76 \mu\text{m}$ along with agglomerates of fine grains. (c,d) sintered at 1020°C, showing same morphology with an average grain size of $3.86 \mu\text{m}$ together with agglomerates of fine grains.

K, 69.09 wt% Nb and 1.62 wt% Si. In Fig 4(c,d), EDS detected 29.33 wt% K and 70.66 wt% Nb in the cubic grain labeled as "D", 29.87 wt% K and 71.13 wt% Nb in cuboidal grains labeled as "F" and 28.62 wt% K, 65.28 wt% Nb and 6.10 wt% Si in agglomerates of fine grains labeled as "E". Furthermore, the EDS analysis of the white spot on regular shaped grain, marked by an arrow in Fig. 3(b), revealed 30.51 wt% K and 69.49 wt% Nb. The observed compositions in EDS analysis are consistent with XRD finding. The edges of the grains containing K, Nb, and Si appeared less sharp or diffused in comparison to those containing K and Nb only, indicating the inhomogeneous mixing of Si in the ceramic body.

3.5 Electrical properties

Variation in ϵ_r and $\tan\delta$ as a function of frequency for the $(1-x)KNbO_3 \cdot xP_2O_5$ ($x = 0.03, 0.05$) and $(1-x)KNbO_3 \cdot xSiO_2$ ($x = 0.1$) samples, investigated at room temperature, are shown in Fig. 4. The dielectric constants and $\tan\delta$ were observed to decrease with an increase in frequency as well as concentration of the sintering aids. This behavior can be attributed to various polarization effects. The observed ϵ_r decreased drastically with an increase in frequency while the $\tan\delta$ first decreased and then increased abruptly with increasing frequency, indicating that the material behaved like a conductor at high frequencies[35]. $KNbO_3$ single crystals are known to exhibit a dielectric constant of 137 and correspond to (111) and (100) planes, i.e., parallel to c-axis of its tetragonal unit cell[36]. In comparison to pure $KNbO_3$ single crystals, the

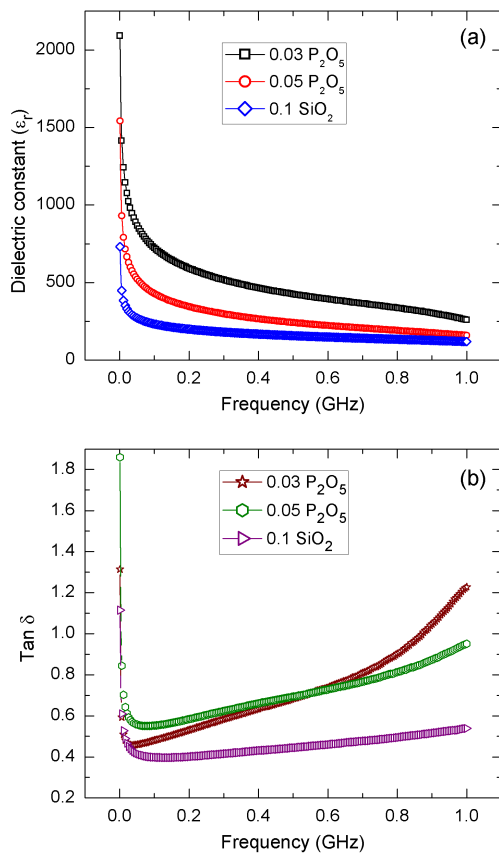


Fig. 4 (a) ϵ_r and (b) $\tan \delta$ measured for $(1-x)KNbO_3 \cdot xP_2O_5$ ($x = 0.03, 0.05$) and $(1-x)KNbO_3 \cdot SiO_2$ ($x = 0.1$) as a function of frequency in the range from 1 MHz to 1 GHz.

compositions under investigation have large values of dielectric constants. The previously reported poor values have been attributed to the presence of potassium and oxygen vacancies as well as the strains produced in these crystals due to evaporation of potassium and oxygen [13]. Hsiang *et al.* [37] reported that electrical properties are density dependent. In the present work, the SiO_2 -added composition was poorly densified and hence deteriorated the electrical properties.

4 Conclusions

In conclusion, we investigated the effects of 0.03 and 0.05 wt% P_2O_5 and 0.1 wt% SiO_2 addition on the phase, microstructure and electrical properties of $KNbO_3$. The values of 81.95 and 84.3% of theoretical density were obtained for stoichiometric KN after sintering at 1000 and 1020 °C for 2 h. The TG/DTA analysis of as-mixed-milled sample showed an overall weight loss of 33.4 wt% in the temperature range of 30-1200 °C. The exothermic behavior, observed at about 795 °C, revealed the beginning of crystallization. The addition of low content P_2O_5 as a dopant resulted in the for-

mation of an unknown secondary phase and promoted the densification of the material. The microstructure of the samples comprised cubic and cuboidal grains with an average grain size of 3.76 μm and 3.86 μm along with agglomerates of fine grains. The grain size increased slightly with an increase in sintering temperature. Dielectric constant and $\tan \delta$ were observed to decrease with an increase in x value as well as frequency.

Acknowledgements

Authors greatly acknowledge the financial support from the Higher Education Commission (HEC) of Pakistan and laboratory support extended by MRL, Department of Physics, University of Peshawar, Pakistan.

References

1. Stefanovich SY, Sigaev VN, Lotarev SV, Lopatina EV, Mosunov AV, Segalla SG, and Chertin DP (2013) Functional Glass Ceramic Based on Potassium Niobate. *Glass and Ceramics* 70:135-140
2. Kim IS, Jung WH, Inaguma Y, Nakamura T, and Itoh M (1995) Dielectric properties of a-site deficient perovskite-type lanthanum-calcium-titanium oxide solid solution system $[(1-x)La_{23}TiO_{3-x}CaTiO_3]$ ($0.1 \leq x \leq 0.96$). *Materials Research Bulletin* 30:307-316
3. Iqbal Y, and Manan A (2012) Phase, microstructure and microwave dielectric properties of Zr-doped $SrLa_4Ti_{5-x}Zr_xO_{17}$. *J Mater Sci: Mater Electron* 23:536-541
4. Sen C, Alkan B, Akin I, Yucel O, Sahin FC, and Goller G (2011) Microstructure and ferroelectric properties of spark plasma sintered Li substituted $K_{0.5}Na_{0.5}NbO_3$ ceramics. *J. Ceram. Soc. Japan* 119:355-361
5. Hertling GH (1999) Ferroelectric Ceramics: History and Technology. *J. Am. Ceram. Soc.* 82:797-818
6. Jaffe H (1958) Piezoelectric Ceramics. *J. Am. Ceram. Soc.* 41:494-498
7. Wu SY, Zhang W, and Chen XM (2010) Formation mechanism of $NaNbO_3$ powders during hydrothermal synthesis. *J Mater Sci: Mater Electron* 21:450-455
8. Ringgaard E, and Wurlitzer T (2005) Lead-free piezoceramics based on alkali niobates. *J. Euro. Ceram. Soc.* 25:2701-2706
9. Shrout TR, and Zhang SJ (2007) Lead-free piezoelectric ceramics: Alternatives for PZT? *J Electroceram* 19:113-126
10. Günter P (1974) Electro-optical properties of $KNbO_3$. *Optics Communications* 11:285-290
11. Uematsu Y (1974) Nonlinear Optical Properties of $KNbO_3$ Single Crystal in the Orthorhombic Phase. *Jpn. J. Appl. Phys.* 13:1362-1368
12. Günter P (1982) Holography, coherent light amplification and optical phase conjugation with photorefractive materials. *Physics Reports* 93:199-299
13. Simões AZ, Ries A, Riccardi CS, Gonzalez AH, Zaghete MA, Stojanovic BD, Cilense M, and Varela JA (2004) Potassium niobate thin films prepared through polymeric precursor method. *Materials Letters* 58:2537-2540
14. Maeder MD, Damjanovic D, and Setter N (2004) Lead Free Piezoelectric Materials. *J. Electroceram.* 13:385-392
15. Saito Y, Takao H, Tani T, Nonoyama T, Takatori K, Homma T, Nagaya T, and Nakamura M (2004) Lead-free piezoceramics. *Nature* 432:84-87

16. Egerton L, and Dillon DM (1959) Piezoelectric and Dielectric Properties of Ceramics in the System Potassium-Sodium Niobate. *J. Am. Ceram. Soc.* 42:438-442
17. Magrez A, Vasco E, Seo JW, Dieker C, Setter N, and Forr L (2006) Growth of Single-Crystalline KNbO₃ Nanostructures. *J. Phy. Chem. B* 110:58-61
18. Liu JF, Li XL, and Li YD (2003) Synthesis and characterization of nanocrystalline niobates. *Journal of Crystal Growth* 247:419-424
19. Jaeger RE, and Egerton L (1962) Hot Pressing of Potassium-Sodium Niobates. *J. Am. Ceram. Soc.* 45:209-213
20. Wang R, Xie R, Sekiya T, Shimojo Y, Akimune Y, Hirosaki N, and Itoh M (2002) Piezoelectric Properties of Spark-Plasma-Sintered (Na_{0.5}K_{0.5})NbO₃PbTiO₃ Ceramics. *Jpn. J. Appl. Phys.* 41:7119-7122
21. Reisman A, Holtzberg F, Triebwasser S, and Berkenblit M (1956) Preparation of Pure Potassium Metaniobate. *J. Am. Chem. Soc.* 78:719-720
22. Zuo R, Rödel J, Chen R, and Li L (2006) Sintering and Electrical Properties of Lead-Free Na_{0.5}K_{0.5}NbO₃ Piezoelectric Ceramics. *J. Am. Chem. Soc.* 89:2010-2015
23. Gao D, Kwok KW, Lin D, and Chan HLW (2009) Microstructure, electrical properties of CeO₂-doped (K_{0.5}Na_{0.5})NbO₃ lead-free piezoelectric ceramics. *Journal of Materials Science* 44:2466-2470
24. Yang MR, Tsai CC, Hong CS, Chu SY, and Yang SL (2010) Piezoelectric and ferroelectric properties of CN-doped K_{0.5}Na_{0.5}NbO₃ lead-free ceramics. *J. Appl. Phys.* 108:094103-094108
25. Su S, Zuo R, Wang X, and Li L (2010) Sintering, microstructure and piezoelectric properties of CuO and SnO₂ co-modified sodium potassium niobate ceramics. *Materials Research Bulletin* 45:124-128
26. Makovec D, Pribošič I, and Drogenik M (2008) TiO₂ as a sintering additive for KNbO₃ ceramics. *Ceramics International* 34:89-94
27. Hao J, Xu Z, Chu R, Zhang Y, Li G, and Yin Q (2009) Effects of MnO₂ on phase structure, microstructure and electrical properties of (K_{0.5}Na_{0.5})_{0.94}Li_{0.06}NbO₃ lead-free ceramics. *Materials Chemistry and Physics* 118:229-233
28. Alkoy EM, and Papila M (2010) Microstructural features and electrical properties of copper oxide added potassium sodium niobate ceramics. *Ceramics International* 36:1921-1927
29. Kosec M, and Kolar D (1975) On activated sintering and electrical properties of NaKNbO₃. *Materials Research Bulletin* 10:335-339
30. Acker J, Kungl H, and Hoffmann MJ (2010) Influence of Alkaline and Niobium Excess on Sintering and Microstructure of Sodium-Potassium Niobate (K_{0.5}Na_{0.5})NbO₃. *Journal of the American Ceramic Society* 93, 1270-1281
31. Chaiyo N, Ruangphanit A, Muanghlua R, Niemcharoen S, Boonchom B, and Vittayakorn N (2011) Synthesis of potassium niobate (KNbO₃) nano-powder by a modified solid-state reaction. *Journal of Materials Science* 46:1585-1590
32. Huang T, Chang YS, Chen GJ, and Chang YH (2007) Preparation and structures of the La_{1-x}K_xCo_{1-x}Nb_xO₃ (x = 0-1) system. *Journal of Alloys and Compounds* 430:205-211
33. Ko JB, and Hong J H, (2010) Structural and thermal properties of potassium niobate glasses for an application in electro-optical product design and manufacture. *J. Ceram. Process. Res* 11:116-119
34. Zhou H, Zheng S, Zhang Y (2004) A new way of synthesis of non-linear optical potassium niobate powder. *J. Mater. Sci* 39, 4359-4361
35. Mansour SF (2005) Frequency and Composition Dependence on the Dielectric Properties for Mg-Zn Ferrite. *Egypt. J. Solids* 28:263-273
36. Rou SH, Hren PD, Hren JJ, Graettinger TM, Ameen MS, Auciello OH, and Kingon AI (1990) High Resolution Imaging of Twin and Antiphase Domain Boundaries in Perovskite KNbO₃ Thin Films. *MRS Proceedings* 183:285-290
37. Hsiang HI, Hsi CS, Huang CC, and Fu SL (2008) Sintering behavior and dielectric properties of BaTiO₃ ceramics with glass addition for internal capacitor of LTCC. *Journal of Alloys and Compounds* 459:307-310